Molecular Biology of the Cell
Vol. 10, 2251–2264, July 1999

The Plant Vesicle-associated SNARE AtVTI1a Likely Mediates Vesicle Transport from the *Trans*-Golgi Network to the Prevacuolar Compartment

Haiyan Zheng,*† Gabriele Fischer von Mollard,†‡§ Valentina Kovaleva,* Tom H. Stevens,‡ and Natasha V. Raikhel*‖

*Department of Energy-Plant Research Laboratory, Michigan State University, East Lansing, Michigan 48824; and ‡Institute of Molecular Biology, University of Oregon, Eugene, Oregon 97403-1229

Submitted February 4, 1999; Accepted April 23, 1999
Monitoring Editor: Chris Kaiser

Membrane traffic in eukaryotic cells relies on recognition between v-SNAREs on transport vesicles and t-SNAREs on target membranes. Here we report the identification of AtVTI1a and AtVTI1b, two *Arabidopsis* homologues of the yeast v-SNARE Vti1p, which is required for multiple transport steps in yeast. AtVTI1a and AtVTI1b share 60% amino acid identity with one another and are 32 and 30% identical to the yeast protein, respectively. By suppressing defects found in specific strains of yeast *vti1* temperature-sensitive mutants, we show that AtVTI1a can substitute for Vti1p in Golgi-to-prevacuolar compartment (PVC) transport, whereas AtVTI1b substitutes in two alternative pathways: the vacuolar import of alkaline phosphatase and the so-called cytosol-to-vacuole pathway used by aminopeptidase I. Both AtVTI1a and AtVTI1b are expressed in all major organs of *Arabidopsis*. Using subcellular fractionation and immunoelectron microscopy, we show that AtVTI1a colocalizes with the putative vacuolar cargo receptor AtELP on the *trans*-Golgi network and the PVC. AtVTI1a also colocalizes with the t-SNARE AtPEP12p to the PVC. In addition, AtVTI1a and AtPEP12p can be coimmunoprecipitated from plant cell extracts. We propose that AtVTI1a functions as a v-SNARE responsible for targeting AtELP-containing vesicles from the *trans*-Golgi network to the PVC, and that AtVTI1b is involved in a different membrane transport process.

INTRODUCTION

In the secretory and endocytic pathways, the movement of proteins and membranes from one location to another relies mostly on vesicular transport. One fundamental question is how the vesicles recognize the correct target membrane. The SNARE hypothesis offers a widely accepted explanation of the mechanism of specificity in vesicle targeting (Söllner *et al.*, 1993). SNAREs (SNAP receptors) are membrane proteins found on both transport vesicles (v-SNARE) and target organelles (t-SNARE). The specific interactions between t- and v-SNAREs ensure that vesicles are targeted to the correct compartment and lead to membrane fusion. The best-characterized SNARE complex consists of syntaxin, SNAP25 (t-SNAREs on the presynaptic membrane), and VAMP-1/synaptobrevin (v-SNARE on synaptic vesicles); it is involved in synaptic vesicle exocytosis (Hanson *et al.*, 1997; Sutton *et al.*, 1998). Homologues of these SNAREs are found to be involved in intracellular vesicle transport processes in yeast and mammalian systems, further supporting this hypothesis (for review, see Hay and Scheller, 1997). Several t-SNAREs have been found in plant cells recently (Bassham *et al.*, 1995; Lukowitz *et al.*, 1996; Sato *et al.*, 1997; Zheng *et al.*, 1999), suggesting that the SNARE hypothesis also applies to plant cells.

Much of our knowledge about vesicular transport to the vacuole has been gained from yeast studies. Several pathways to the yeast vacuole have been de-

† These authors contributed equally to this work.
§ Present address: Georg-August-University, Biochemie II, Göttingen, Germany 37073.
‖ Corresponding author. E-mail address: nraikhel@pilot.msu.edu.

scribed. The best characterized pathway for delivery of soluble proteins to the vacuole is the carboxypeptidase Y (CPY) pathway. At the *trans*-Golgi or *trans*-Golgi network (TGN), CPY is bound by its receptor (Pep1p/Vps10p) and packaged into transport vesicles. These vesicles then fuse with the prevacuolar compartment (PVC)/late endosome. The PVC t-SNARE Pep12p is required for correct sorting of CPY (Becherer *et al.*, 1996; Jones, 1977). The v-SNARE Vti1p interacts both genetically and biochemically with Pep12p (Fischer von Mollard *et al.*, 1997). It was thus proposed that Vti1p and Pep12p form a SNARE complex that is involved in docking and fusion of TGN-derived transport vesicles with the PVC. It has recently been reported that a subset of proteins, including alkaline phosphatase (ALP), is transported to the vacuole by an alternative route, independent of the CPY pathway, that bypasses the PVC (Cowles *et al.*, 1997b; Piper *et al.*, 1997). This transport pathway requires the adaptor complex AP-3 (Cowles *et al.*, 1997a; Stepp *et al.*, 1997) and Vam3p, the vacuolar t-SNARE (Darsow *et al.*, 1997; Piper *et al.*, 1997; Wada *et al.*, 1997; Srivastava and Jones, 1998). Vti1p has very recently been implicated as the v-SNARE that interacts with Vam3p in the ALP pathway to the yeast vacuole (Fischer von Mollard and Stevens, 1999). Another route to the vacuole, directly from the cytoplasm, has recently been analyzed using the hydrolase aminopeptidase I (API) (Klionsky, 1998). This cytosol-to-vacuole transport (CVT) pathway is blocked in *vam3* mutant cells (Darsow *et al.*, 1997; Srivastava and Jones, 1998) as well as in *vti1* mutant cells (Fischer von Mollard and Stevens, 1999). Thus, in yeast, multiple pathways are used for delivering vacuolar proteins, all of which require Vti1p. In addition to a role in transport pathways to the vacuole, Vti1p also functions in retrograde transport within the Golgi complex by interacting with the *cis*-Golgi t-SNARE Sed5p (Fischer von Mollard *et al.*, 1997; Lupashin *et al.*, 1997). Furthermore, Holthuis *et al.* (1998) reported the biochemical interaction of Vti1p with two additional yeast Golgi/endosomal t-SNAREs, Tlg1p and Tlg2p. Taken together, these data suggest that Vti1p is a v-SNARE involved in multiple membrane transport pathways in yeast.

In plants, three types of vacuolar sorting signals (VSSs) have been identified (for review, see Bassham and Raikhel, 1997). These VSSs can occur in the form of a propeptide (either N-terminal or C-terminal) that is removed proteolytically during or after transport to the vacuole, or they can form a part of the mature protein. Interestingly, plant vacuolar proteins with N-terminal and C-terminal VSSs appear to use independent pathways (Matsuoka *et al.*, 1995). Although very little information is available on the targeting signals of tonoplast proteins in plants, it is known that they are transported by a different mechanism than that of soluble vacuolar proteins (Gomez and Chrispeels, 1993). Several components of the plant secretory machinery have been isolated as well. In *Arabidopsis*, a Pep12p homologue, AtPEP12p, is found by its ability to complement a yeast *pep12* mutant (Bassham *et al.*, 1995). AtPEP12p is localized to a novel compartment by electron microscopy (EM) and biochemical analysis (Conceição *et al.*, 1997; Sanderfoot *et al.*, 1998). AtELP was identified in *Arabidopsis* by its structural similarity to the EGF receptor and other cargo receptors (Ahmed *et al.*, 1997). AtELP is enriched in clathrin-coated vesicles (CCVs); it has been localized to the TGN and colocalized with AtPEP12p on the PVC by EM (Ahmed *et al.*, 1997; Sanderfoot *et al.*, 1998). AtELP is homologous to BP-80, a protein from pea CCVs that has been shown to bind a broad range of plant VSSs, but not to the C-terminal VSSs (Kirsch *et al.*, 1994, 1996). Recently, another AtELP homologue from pumpkin has been found to recognize certain sequence patches in some cargo proteins (Shimada *et al.*, 1997). All of these data support the notion that AtELP is a cargo receptor involved in transport of some but not all vacuolar proteins. It is postulated that the compartment where AtPEP12p resides is the equivalent of the PVC in yeast or the late endosome in mammalian cells. This compartment accepts the transport vesicles formed at the TGN as CCVs. Those vesicles contain at least a subset of vacuolar proteins and the receptors (such as AtELP) involved in packaging them at the TGN.

We have identified two *Arabidopsis* genes (*AtVTI1a* and *AtVTI1b*) encoding proteins homologous to yeast Vti1p. Although each *Arabidopsis VTI1* gene can function in yeast, they function in different sorting pathways to the yeast vacuole. By studying T7 epitope-tagged AtVTI1a, we found that AtVTI1a colocalized with the putative vacuolar cargo receptor AtELP on the TGN and the PVC and with AtPEP12p on the PVC. Coimmunoprecipitation of AtVTI1a with AtPEP12p suggested that these two proteins associate in the cell. Thus, we propose that AtVTI1a is a plant v-SNARE involved in the transport of vacuolar cargo from the Golgi to the PVC.

MATERIALS AND METHODS

Plasmids, Yeast Strains, and Growth Media

Mutant strains of *vti1* were derived from the yeast strains SEY6210 (*MATα leu2-3112 ura3-52 his3-Δ200 trp1-Δ901 lys2-801 suc2-Δ9 mel*$^-$) and SEY6211 (*MATα leu2-3112 ura3-52 his3-Δ200 trp1-Δ901 ade2-101 suc2-Δ9 mel*$^-$)(Robinson *et al.*, 1988). The strains *vti1Δ* (FvMY6), *vti1-1* (FvMY7), *vti1-2* (FvMY24), and *vti1-11* (FvMY21) and the *GAL1-VTI1* plasmid (pFvM16) have been described earlier (Fischer von Mollard *et al.*, 1997; Fischer von Mollard and Stevens, 1998). The *vti1Δ* yeast strain (FvMY6) was propagated carrying the *GAL1-VTI1* plasmid (pFvM16) in the presence of galactose, because the *vti1Δ* mutation is lethal to yeast cells.

To express AtVTI1a and AtVTI1b in yeast, *Bam*HI and *Pst*I sites were introduced by PCR into *AtVTI1a* and *AtVTI1b* cDNAs flanking

the start and stop codons. The *Bam*HI and *Pst*I fragments were inserted into the yeast expression vector pVT102U (Vernet *et al.*, 1987). To construct N-terminal T7-tagged AtVTI1a, *Bam*HI and *Sal*I sites were generated by PCR flanking the *AtVTI1a* ORF. The *Bam*HI–*Sal*I fragment of *AtVTI1a* was then inserted into the same sites of pET21a (Novagen, Madison, WI) to create a T7-N-terminal fusion of AtVTI1a (pETT7-AtVTI1a). The *T7-AtVTI1a* fragment was then subcloned into the *Xba*I and *Xho*I sites of the pVT102U vector for yeast expression. To construct pBI-T7-AtVTI1a for plant transformation, the *Xba*I–*Sac*I fragment of pETT7-AtVTI1a was subcloned into pBI121 (Clontech, Palo Alto, CA). For *Escherichia coli* overexpression of 6xHis-AtVTI1a, the *Nde*I site at the ATG start codon and the *Bam*HI site immediately downstream of the cytoplasmic domain were introduced by PCR amplification. The *Nde*I–*Bam*HI fragment of *AtVTI1a* was then subcloned into pET14b (Novagen) and transformed into *E. coli* BL21(DE3) cells for overexpression.

Yeast strains were grown in rich medium (YEPD) or standard minimal medium (SD) with appropriate supplements (Fischer von Mollard *et al.*, 1997). To induce expression from the *GAL1* promoter, dextrose was replaced by 2% raffinose and 2% galactose.

Immunoprecipitation of ^{35}S-labeled Yeast Proteins

CPY, ALP, and API were immunoprecipitated as described earlier (Klionsky *et al.*, 1992; Vater *et al.*, 1992; Nothwehr *et al.*, 1993). SEY6211 wild-type cells and *vti1* mutant cells were grown at 24°C and preincubated for 15 min at 36°C before labeling at 36°C.

For CPY immunoprecipitations, log-phase growing yeast cells were labeled for 10 min with ^{35}S-Express (DuPont-New England Nuclear, Boston, MA) label (10 μl/0.5 OD unit of cells at 600 nm) followed by a 30-min chase with cysteine and methionine. The medium was separated, and the cell pellet was spheroplasted and lysed. CPY was immunoprecipitated from the medium and cellular extracts. For ALP immunoprecipitations, yeast cells were labeled for 7 min and chased for 30 min. The cell pellet was spheroplasted. The spheroplast pellet was extracted with 50 μl of 1% SDS and 8 M urea at 95°C and diluted with 950 μl of 90 mM Tris-HCl, pH 8.0, 0.1% Triton X-100, and 2 mM EDTA; the supernatant was used for immunoprecipitations. To investigate API traffic, 0.25 OD unit (at 600 nm) of yeast cells in 500 μl of medium were labeled with 10 μl of ^{35}S-Express label for each time point. After a 10-min pulse, cells were chased for 120 min. The cell pellet was spheroplasted. Extracts for immunoprecipitations were prepared from spheroplast pellets by boiling in 50 μl of 50 mM sodium phosphate, pH 7.0, 1% SDS, and 3 M urea and diluted with 950 μl of 50 mM Tris-HCl, pH 7.5, 0.5% Triton X-100, 150 mM NaCl, and 0.1 mM EDTA. The API antiserum was kindly provided by D. Klionsky (University of California, Davis, CA). Immunocomplexes were precipitated using fixed cells of *Staphylococcus aureus* (IgGsorb). Immunoprecipitates were analyzed by SDS-PAGE and autoradiography.

RNA Preparation from Arabidopsis

Total RNA extraction from different plant organs was performed based on the method of Bar-Peled and Raikhel (1997), except that the RNA was further purified by phenol:chloroform:isoamyl alcohol (25:24:1, vol/vol/vol) and chloroform:isoamyl alcohol (24:1, vol/vol) extraction followed by ethanol precipitation. Purified total RNA from 1 g of tissue was resuspended in 200 μl of diethylpyrocarbonate-treated water. The concentration of the RNA was determined by the OD_{260} value.

5′-Rapid Amplification of cDNA 5′ Ends (RACE)

5′ RACE was performed according to the manufacturer's (Life Technologies, Gaithersburg, MD) instruction. Total RNA (0.5 μg) from *Arabidopsis* roots was used as a template, and the required amount of primer 1 (5′-GTG AGT TTG AAG TAC AA-3′) was used for the first-strand cDNA synthesis. 5′-RACE abridged anchor primer supplied by the manufacturer was used as a sense primer. Primer 2 (5′-TGC GAT GAT GAT GGC TCC AA-3′) and primer 3 (5′-GTT CAT CCT CCT CGT CAT-3′) were used as antisense primers for the first round and the following nested PCR reactions, respectively. DNA fragments produced from nested PCR were end blunted, cloned into Bluescript SK(−) (Stratagene, La Jolla, CA), and manually sequenced using Sequenase version 2.0 (United States Biochemical, Cleveland, OH).

RNA Blot Analysis

For Northern analysis, 20 μg of *Arabidopsis* total RNA were applied to each lane of a formaldehyde denaturing agarose gel and separated as described by Sambrook *et al.* (1989). Separated RNA was then transferred to a Hybond-N (Amersham, Buckinghamshire, England) nylon membrane. For dot blot analysis, various amounts of in vitro–transcribed mRNA were applied to a Hybond-N membrane. Blots were hybridized with [^{32}P]UTP-labeled RNA probes.

Antibody Production

6XHis-tagged AtVTI1a was overexpressed by isopropyl-1-thio-β-D-galactopyranoside induction. The His-tagged protein was purified by passing through a His-Bind column (Novagen, Madison, WI). The purified protein was then injected into a guinea pig for antibody production. AtPEP12p rabbit antiserum and preimmune serum were described by Conceição *et al.* (1997). AtELP rabbit antiserum and preimmune serum were described by Ahmed *et al.* (1997). H^+-pyrophosphatase (H^+PPase) antibody is a gift from Dr. S. Yoshida (Hokkaido University, Sapporo, Japan) and was described by Maeshima and Yoshida (1989).

Subcellular Fractionation

To fractionate subcellular compartments based on their mass, differential centrifugation was performed as follows: 0.5 g of *Arabidopsis* root cultures (21 d old) were homogenized in 1 ml of extraction buffer (50 mM HEPES-KOH, pH 7.5, 10 mM KOAc, 1 mM EDTA, 0.4 M sucrose, 1 mM DTT, and 0.1 mM PMSF). The lysate was centrifuged at 4°C, 1000 × *g*, for 10 min. The pellet was discarded, and the supernatant (S1) was then centrifuged at 4°C, 8000 × *g*, for 20 min. The pellet (P8) was resuspended in 200 μl of 2× Laemmli loading buffer. This supernatant was ultracentrifuged at 4°C, 100,000 × *g*, for 2 h. The pellet (P100) was resuspended in 200 μl of 2× Laemmli loading buffer. The supernatant (S100), P8, and P100 were analyzed by SDS-PAGE, followed by immunoblotting using different antibodies.

Based on density differences, the microsomes were separated on a step sucrose gradient as described by Sanderfoot *et al.* (1998).

Arabidopsis Transformation

pBI-T7-AtVTI1a was introduced into *Agrobacterium tumefaciens* LBA4404 by $CaCl_2$-based transformation. *Arabidopsis* Columbia plants were transformed using vacuum infiltration as described by Bent *et al.* (1994). Transformants were selected by kanamycin, and the presence of T7-AtVTI1a was detected in several independent lines by protein gel blot analysis using T7 mAb (Novagen) and guinea pig polyclonal antiserum against AtVTI1a.

EM Procedure

The root tips of *Arabidopsis* plants transformed with T7-AtVTI1a were fixed in a buffer containing 1.5% formaldehyde, 0.5% glutaraldehyde, and 0.05 M sodium phosphate, pH 7.4 for 2.5 h at room temperature. The specimens were rinsed in the same buffer and postfixed in 0.5% OsO_4 for 1 h at room temperature. Dehydrated specimens were embedded in London Resin White (Polysciences, Warrington, PA). Ultrathin sections were made with an Ultracut S

microtome (Reichert-Jung, Vienna, Austria) by a diamond knife and collected on nickel grids precoated with 0.25% Formvar.

For immunolabeling, the protocol according to Sanderfoot *et al.* (1998) was used with small modification. Primary mouse mAb against T7 epitope tag (Novagen) were detected by rabbit anti-mouse IgG for 1 h, followed by biotinylated goat anti-rabbit IgG for 1 h, and then by streptavidin conjugated to 10-nm colloidal gold particles. For double labeling, the grids were first treated as above for T7 tag antibody, and then a second fixation step using 0.1% glutaraldehyde, followed by a second blocking step with 2% BSA in PBST (PBS and 0.1% Tween 20) to prevent cross-reactivity of the T7 tag-antibody in later steps (Slot *et al.*, 1991). The grids were then incubated with specific rabbit antiserum for AtELP for 4 h, followed by a 1-h incubation with biotinylated goat anti-rabbit IgG and then by streptavidin conjugated to 5-nm colloidal gold particles. The control sections were treated with 2% BSA in PBST instead of antibody against the T7 tag and with the AtELP preimmune serum. The grids were washed in distilled water and stained with 2% uranyl acetate in H_2O for 30 min and lead citrate for 10 min (Reynold's solution). The sections were examined with a Philips (Eindoven, the Netherlands) CM 10 transmission electron microscope. All labeling experiments were conducted several times each on independent sections. Fifty Golgi complexes were analyzed for AtVTI1a distribution, and 40 complexes were analyzed for double immunolabeling of AtVTI1a and AtELP.

Cryosections of *Arabidopsis* roots were used for double labeling of AtVTI1a and AtPEP12p. The sectioning procedure was described by Sanderfoot *et al.* (1998). Immunolabeling was also performed as described by Sanderfoot *et al.* (1998) with some modifications. T7-AtVTI1a localization was detected as described above when London Resin White sections were used and visualized with 10-nm colloidal gold. AtPEP12p was detected using AtPEP12p antiserum and visualized with 5-nm colloidal gold. For final embedding, the grids were washed and stained by a mixture of polyvinyl alcohol and uranyl acetate according to the method of Tokuyasu (1989).

Immunopurification of T7-AtVTI1a from Plant Extract

Three grams of 21-d-old plants were homogenized on ice in 6 ml of extraction buffer (50 mM HEPES-KOH, pH 6.5, 10 mM potassium acetate, 100 mM sodium chloride, 5 mM EDTA, and 0.4 M sucrose) with protease inhibitor mixture (100 μM PMSF, 1 μM pepstatin, 0.3 μM aprotinin, and 20 μM leupeptin). The debris was pelleted by centrifugation at 1000 $\times$ *g* for 10 min. Triton X-100 was added to the supernatant to a final concentration of 1% to solubilize membrane proteins. This solubilized protein extract was incubated with 50 μl of T7 tag antibody agarose (Novagen) at 4°C for 5 h. The agarose was then collected by centrifugation at 4°C, 500 $\times$ *g*, for 1 min and washed five times in extraction buffer with 1% Triton X-100. Protein purified by T7 tag antibody agarose was then eluted in 50 μl of 2$\times$ Laemmli buffer. Equal volumes of total protein extract, flow-through, or eluate were separated on SDS-PAGE followed by immunoblotting using different antibodies.

RESULTS

There Are Two Highly Similar AtVTI1 Genes Found in Arabidopsis

A search of the *Arabidopsis* expressed sequence tag (EST) database using the Blast program (Altschul *et al.*, 1990) resulted in a partial sequence that showed similarity to yeast Vti1p. 5′-RACE was performed to obtain the upstream sequence of this cDNA. With this 5′-RACE sequence, the *Arabidopsis* EST database was searched again, and two sets of EST clones were found. The clone (accession number T14238) containing an ORF of 221 amino acids was termed *AtVTI1a*. The clone (accession number T75644) containing an ORF of 224 amino acids was termed *AtVTI1b* (Figure 1). These two genes share similarity at the nucleotide sequence level (58.4% identity) and the deduced amino acid sequence level (59.5% identity; see Table 1). Hydropathy analysis (Kyte and Doolittle, 1982) predicted similar structures for AtVTI1a and AtVTI1b proteins (our unpublished results). The sequences predicted hydrophilic proteins with a short hydrophobic region at their extreme C termini (Figure 1, underlined), possibly serving as a membrane anchor. The region immediately preceding the probable membrane-spanning domain contains two heptad repeat structures that would potentially form amphiphilic alpha helices. Predicted amino acid sequences of these two AtVTI1 and Vti1 proteins found in other organisms were compared using the J. Hein method in the MegAlign program (DNAStar software package) (Figure 1 and Table 1). The alignment showed that Vti1 proteins exhibit significant similarities among yeast, mammals, and plants (yVti1p and AtVTI1a, 32.4% identical; yVti1p and AtVTI1b, 30.8% identical; yVti1p and hVti1p, 23.9% identical; yVti1p and mVti1a, 33.8% identical; yVti1p and mVti1b, 23.5% identical). All Vti1 proteins have a short hydrophobic region at the C terminus. The most conserved amino acid residues among Vti1 proteins are concentrated in the heptad repeat region next to the transmembrane domain, a region thought to be involved in interaction between t- and v-SNAREs (Calakos *et al.*, 1994; Hayashi *et al.*, 1994; Fischer von Mollard and Stevens, 1998).

AtVTI1a and AtVTI1b Function in Different Trafficking Steps in Yeast

Next, we investigated whether either AtVTI1a or AtVTI1b could functionally replace the yeast Vti1p in various membrane trafficking steps in yeast. For this purpose the coding sequences of *AtVTI1a* or *AtVTI1b* were cloned into a multicopy yeast expression vector behind the *ADH1* promoter. In yeast the *VTI1* gene is essential for cell growth. Therefore, we determined whether expression of the *Arabidopsis* Vti1 homologues would allow yeast cells to grow in the absence of the yeast Vti1p. The expression of yeast *VTI1* was placed under the control of the *GAL1* promoter. These cells (FvMY6/pFvM16) were able to divide on galactose plates (Figure 2A, Gal), but not on glucose plates (Glc). Expression of either AtVTI1a or AtVTI1b allowed for growth on glucose medium. Cells expressing AtVTI1b grew more slowly than cells expressing AtVTI1a. *vti1*Δ cells (FvMY6) expressing AtVTI1a divided with a doubling time of 3.5 h, and *vti1*Δ cells expressing AtVTI1b had a doubling time of ~8 h, compared with 2.5 h for wild-type cells (our unpub-

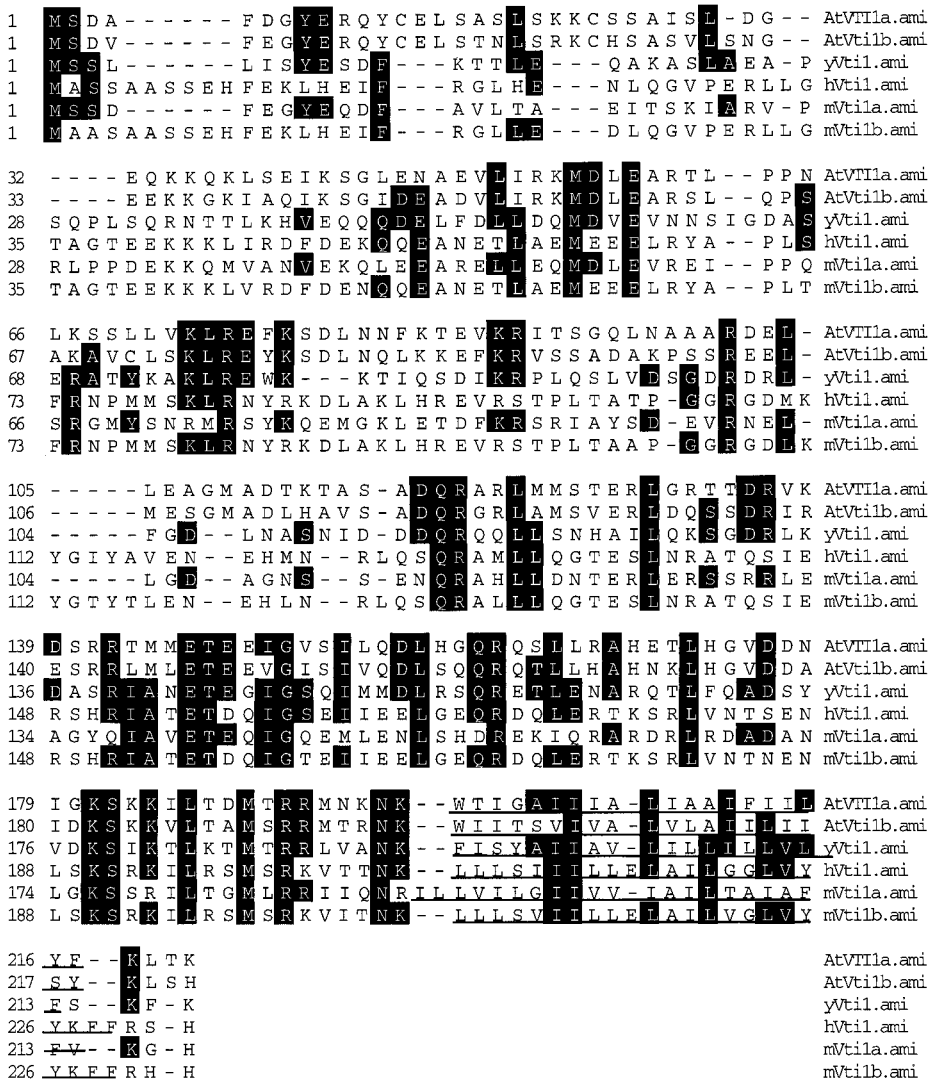

Figure 1. Sequence comparison of AtVTI1a and AtVTI1b with other members of the family including yVti1p (*Saccharomyces cerevisiae*, accession number 2497184), hVti1p (*Homo sapiens*, accession number 268740), mVti1a (*Mus musculus*, accession number 3213227), and mVti1b (*Mus musculus*, accession number 3213229). The sequence comparison was generated using the J. Hein method in MegAlign (DNAStar program). Amino acids identical to yVti1p are shaded in black. The C-terminal hydrophobic domain is underlined.

lished results). These data indicate that either AtVTI1a or AtVTI1b could replace yeast Vti1p in its essential function, although to different extents.

Various membrane trafficking steps in yeast can be analyzed by following the fate of newly synthesized proteins in experiments involving pulse–chase labeling with ^{35}S followed by immunoprecipitation. The soluble vacuolar hydrolase CPY is glycosylated in the endoplasmic reticulum to produce the p1CPY precursor (Stevens *et al.*, 1982). Further modification in the Golgi apparatus gives rise to p2CPY. CPY is sorted in the TGN and transported from there through the prevacuolar/endosomal compartment (PVC) to the vacuole and then cleaved to the mature mCPY (Bryant and Stevens, 1998). Transport from the Golgi to the PVC is blocked in the temperature-sensitive *vti1-1* cells (Fischer von Mollard *et al.*, 1997). Compared with wild-type yeast, in which CPY was retained in the vacuole as mature form (Figure 2B, lane 1), the *vti1-1* cells (FvMY7) accumulated p2CPY within the cell (lane 3) and secreted p2CPY (lane 4) at the nonpermissive temperature. As indicated by the prevalence of mCPY (lane 5), CPY was transported to the vacuole in *vti1-1* cells expressing AtVTI1a as effectively as in wild-type cells. By contrast, only low amounts of mCPY were found in *vti1-1* cells expressing AtVTI1b (lane 7), and most of the CPY was secreted (lane 8). *vti1-11* cells (FvMY21) accumulated p1CPY at the re-

Table 1. Relative sequence identity between Vti1 protein homologues

	AtVTI1a	AtVTI1b	yVti1p	hVti1p	mVti1a	mVti1b
AtVTI1a	100	59.9	32.4	26.7	33.3	28.1
AtVTI1b		100	30.8	27.5	31.8	28.0
yVti1p			100	23.9	33.8	23.5
hVti1p				100	30.1	91.9
mVti1a					100	31.5
mVti1b						100

Amino acid sequence similarity shown as identical sequence percentage. AtVTI1a, AtVTI1b, and yVti1p, *Saccharomyces cerevisiae* (accession number 2497184); HVti1p, *Homo sapiens* (accession number 268740); mVti1a, *Mus musculus* (accession number 3213227); mVTI1b, *Mus musculus* (accession number 3213229). The optimal alignments were produced using the J. Hern method in the DNAStar program.

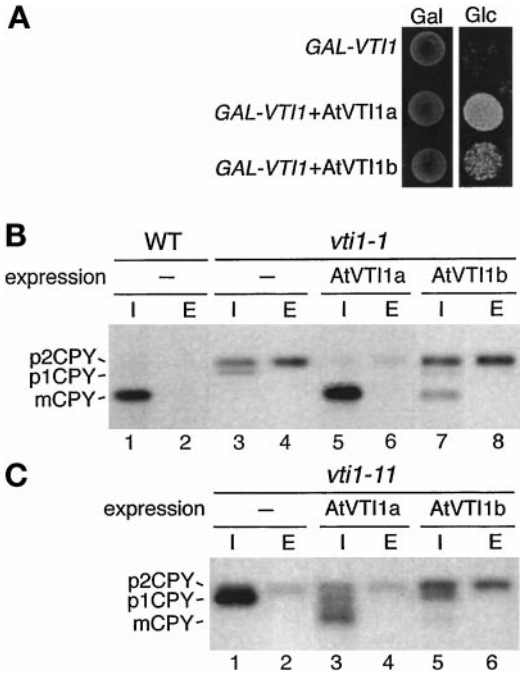

Figure 2. Expression of either AtVTI1a or AtVTI1b allows yeast cells to grow in the absence of Vti1p, but only AtVTI1a functions in TGN-to-PVC traffic. (A) Growth of the *vti1*Δ *GAL1-VTI1* strain (FvMY6/pFvM16) alone or expressing AtVTI1a or AtVTI1b on plates containing galactose (Gal) or glucose (Glc). The *vti1*Δ *GAL1-VTI1* strain could not grow on glucose after the expression of *VTI1* was shut off, but expression of either AtVTI1a or AtVTI1b supported growth. (B and C) CPY traffic in wild-type, *vti1-1* (FvMY7) (B) and *vti1-11* (C) cells (FvMY21) alone (−) or expressing AtVTI1a or AtVTI1b. Cells were grown at 24°C, preincubated at 36°C for 15 min, pulse labeled for 10 min, and chased for 30 min at 36°C. CPY was immunoprecipitated from cellular extracts (I) and extracellular fractions (E) and analyzed by SDS-PAGE and autoradiography. The TGN-to-PVC traffic block in *vti1-1* cells (FvMY7) was suppressed by AtVTI1a expression, as indicated by the presence of vacuolar mCPY, but not by AtVTI1b expression. (C) *vti1-11* cells (FvMY21) accumulated p1CPY because of a block in retrograde traffic to the *cis*-Golgi. Expression of either AtVTI1a or AtVTI1b reduced the amount of p1CPY that accumulated.

strictive temperature (Figure 2C, lane 1) because of a defect in retrograde traffic to the *cis*-Golgi as well as a defect in traffic from the TGN to the PVC (Fischer von Mollard *et al.*, 1997). *vti1-11* cells, but not *vti1-1* cells, display a severe temperature-sensitive growth defect, indicating that retrograde traffic to the Golgi is essential (Fischer von Mollard *et al.*, 1997). Expression of AtVTI1a suppressed the accumulation of p1CPY and resulted in the appearance of mCPY (Figure 2C, lane 3). Expression of AtVTI1b also reduced the amount of p1CPY (lane 5); CPY was not directed to the vacuole but was secreted instead (lane 6). These results indicate that AtVTI1a can replace yeast Vti1p both in transport from the TGN to the PVC (interaction with the t-SNARE Pep12p) and in retrograde traffic to the *cis*-Golgi (interaction with the t-SNARE Sed5p). By contrast, AtVTI1b functions in retrograde traffic to the *cis*-Golgi but not in traffic from the TGN to the PVC.

The vacuolar membrane protein ALP uses a different transport pathway from the TGN to the vacuole and does not travel through the PVC as does CPY (Bryant and Stevens, 1998; Odorizzi *et al.*, 1998). In pulse–chase labeling experiments, arrival at the vacuole is indicated by processing of pALP to mALP (Figure 3A, lane 2) (Klionsky and Emr, 1989). ALP traffic to the vacuole occurs with a half-time of about ~5 min in wild-type cells. *vti1-2* cells (FvMY24) accumulated pALP at the nonpermissive temperature (lane 4), demonstrating that Vti1p is also required for ALP transport (Fischer von Mollard and Stevens, 1999). This trafficking defect was not corrected by expression of AtVTI1a in *vti1-2* cells (lane 6). By contrast, pALP was transported to the vacuole and processed to mALP in *vti1-2* cells expressing AtVTI1b after a 30-min chase period (lane 8), indicating that AtVTI1b functions in ALP traffic to the vacuole.

A third biosynthetic pathway to the vacuole is taken by API. API is synthesized as a cytoplasmic precursor, pAPI, and engulfed by a double membrane that forms CVT vesicles (Klionsky, 1998). These CVT vesicles fuse with the vacuolar membrane, and pAPI is cleaved to vacuolar mAPI (Figure 3B, lane 2). Transport of API

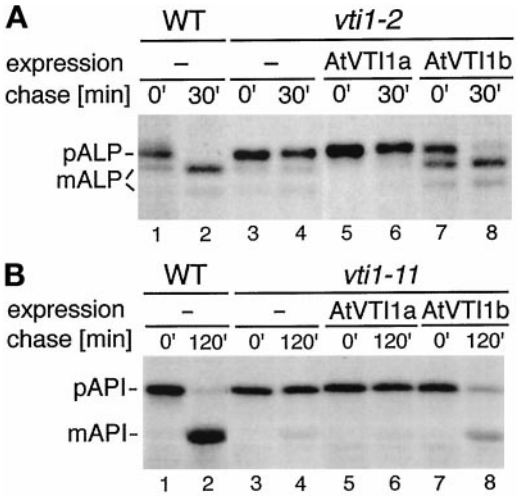

Figure 3. AtVTI1b but not AtVTI1a could replace yeast Vti1p in ALP and API traffic to the vacuole, which are transported to the vacuole via two different biosynthetic pathways. (A) Wild-type and *vti1-2* cells (FvMY24) alone (−) or expressing either AtVTI1a or AtVTI1b were grown at 24°C, preincubated at 36°C for 15 min, pulse labeled for 7 min, and chased for 0 or 30 min at 36°C. ALP was immunoprecipitated from cellular extracts and separated by SDS-PAGE. The accumulation of pALP in *vti1-2* cells was suppressed by expression of AtVTI1b but not by AtVTI1a. (B) Wild-type and *vti1-11* cells (FvMY21) alone (−) or expressing AtVTI1a or AtVTI1b were grown at 24°C, preincubated at 36°C for 15 min, labeled for 10 min, and chased for 0 or 120 min at 36°C. API was immunoprecipitated from cellular extracts and analyzed by SDS-PAGE. Vacuolar mAPI was found only in *vti1-11* cells expressing AtVTI1b, not in *vti1-11* cells expressing AtVTI1a.

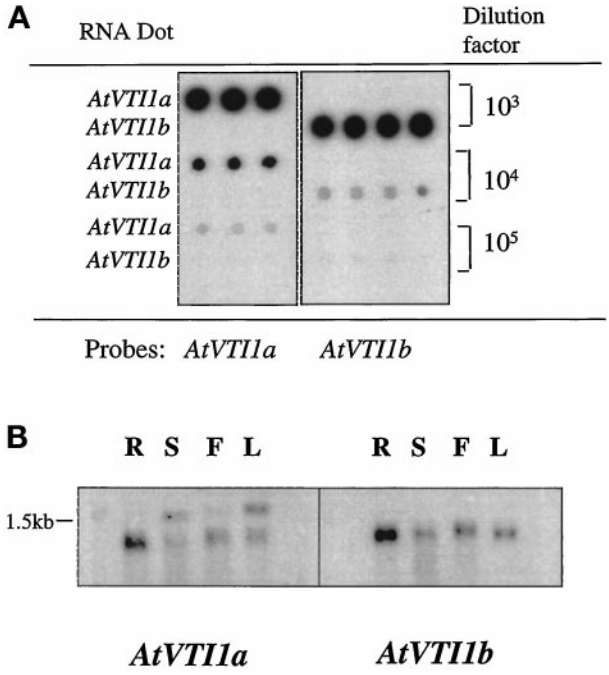

Figure 4. Northern blot analyses of *AtVTI1a* and *AtVTI1b*. (A) Dot blot for testing the specificity of the *AtVTI1a* and *AtVTI1b* probes. One microliter of in vitro–transcribed mRNAs of *AtVTI1a* and *AtVTI1b* in serial 10× dilutions was applied to the Hybond-N membrane and hybridized with in vitro–transcribed [α-^{32}P]UTP-labeled RNA probes at high stringency (65°C for 16 h). The blot was washed under highly stringent conditions (2× SSC and 1% SDS for 30 min at 65°C, 0.2× SSC and 1% SDS 10 min for three times at room temperature). The signal was then detected by autoradiography. (B) RNA gel blot analysis of *AtVTI1* expression in several *Arabidopsis* organs. Twenty micrograms of total RNA extracted from roots (R), stems (S), flowers (F), and leaves (L) were separated on a denaturing gel and transferred to Hybond-N. The membrane was then hybridized with probes described in A following the same procedure.

along this pathway has a half-time of ~45 min. Transport of API was blocked in *vti1-11* cells (FvMY21) at the restrictive temperature (Fischer von Mollard and Stevens, 1999), as indicated by the absence of mAPI after a 120-min chase period (lane 4). Expression of AtVTI1a in *vti1-11* cells did not suppress the API traffic defect (lane 6). As indicated by the presence of mAPI in *vti1-11* cells expressing AtVTI1b (lane 8), AtVTI1b can partially fulfill the function of Vti1p in API traffic along the CVT pathway.

Taken together, these data indicate that whereas AtVTI1a can function in traffic from the TGN to the PVC; AtVTI1a cannot replace Vti1p in traffic along either the ALP or CVT pathway to the vacuole. By contrast, AtVTI1b functions in membrane traffic along the ALP and CVT pathways to the vacuole but not in transport from the TGN to the PVC.

Both AtVTI1a and AtVTI1b Transcripts Are Expressed in All Organs in Arabidopsis

Finding that AtVTI1a and AtVTI1b function in different vacuolar transport pathways in yeast prompted us to analyze their specific distribution in *Arabidopsis* plants. To detect the expression pattern of these *AtVTI1* genes, we performed Northern analysis of various *Arabidopsis* plant organs. Because of the high similarity of *AtVTI1a* and *AtVTI1b*, an untranslated region of each clone was used to prepare gene-specific RNA probes. The specificity of these two probes was first checked by dot blot of in vitro–translated *AtVTI1a* and *AtVTI1b* mRNA, as revealed in Figure 4A. The dot blot of in vitro–transcribed *AtVTI1a* hybridized with the *AtVTI1a* antisense RNA probe. Similarly, in vitro–transcribed *AtVTI1b* hybridized only with the *AtVTI1b* antisense RNA probe. These results demonstrate that the probes are specific under stringent hybridization and washing conditions. These two gene-specific probes were used to hybridize RNA blots of total RNAs from *Arabidopsis* roots, stems, leaves, and flowers. As shown in Figure 4B, *AtVTI1a* and *AtVTI1b* were expressed in all organs investigated. The *AtVTI1a* probe also recognized a band that migrated at ~1.6 kb; however, this band was found to be irrelevant to the *AtVTI1a* gene because another probe to-

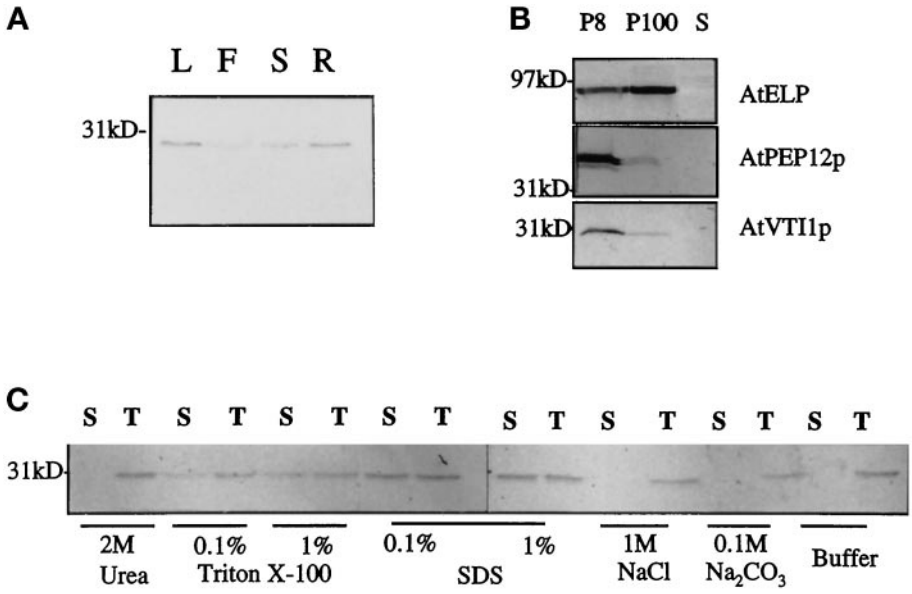

Figure 5. AtVTI1a is an integral membrane protein. (A) Distribution of AtVTI1a in *Arabidopsis* organs. Equal amounts of total protein from leaves (L), flowers (F), stems (S), and roots (R) were separated by SDS-PAGE and immunoblotted with guinea pig antiserum against AtVTI1a. Molecular mass is indicated on the left. (B) AtVTI1a fractionates with heavy membranes during differential centrifugation. A postnuclear supernatant from 0.5 g of cultured roots was centrifuged at 8000 × *g* for 20 min. The pellet (P8) was solubilized in 200 μl of 2× Laemmli loading buffer. The supernatant (S8) was further ultracentrifuged at 100,000 × *g* for 2 h. The pellet (P100) was solubilized in 200 μl of 2× Laemmli buffer. Equal amounts of the supernatant (S100), P100, and P8 were separated by SDS-PAGE and immunoblotted with anti-AtVTI1a, anti-AtELP, or anti-AtPEP12p antiserum. Molecular mass is indicated on the left. (C) AtVTI1a is an integral membrane protein. Equal amounts of total membranes from *Arabidopsis* cultured cells were treated with 2 M urea, 0.1 or 1% Triton X-100, 0.1 or 1% SDS, 1 M NaCl, 0.1 M Na_2CO_3, pH 11, or extraction buffer alone. All treatments were performed at room temperature for 30 min. An aliquot of each treatment was saved as total. Membranes were pelleted by centrifugation at 100,000 × *g* for 1 h after the treatments. Equal volumes of supernatant or total were separated by SDS-PAGE and immunoblotted with anti-AtVTI1a antiserum. S, supernatant, T, total.

ward *AtVTI1a* failed to recognize it (our unpublished results). The mRNA organ distribution patterns of these two genes were similar to each other; however, there was more mRNA in roots than in leaves, a pattern similar to the distribution of *AtPEP12* (Bassham *et al*., 1995) and *AtELP* (Ahmed *et al*., 1997). Thus, we found no variation in distribution of *AtVTI1a* and *AtVTI1b* transcripts among plant organs.

AtVTI1a Is an Integral Membrane Protein

To study the behavior of AtVTI1a, we raised antibodies toward the cytosolic part of this protein in guinea pig. The antisera specifically recognized a 28-kDa band in leaves, roots, stems, and flowers of *Arabidopsis* (Figure 5A). The molecular mass of this band agreed well with the deduced molecular mass of AtVTI1a based on sequence information. The sequence analysis predicted that AtVTI1a, like most other v-SNAREs, has a C-terminal hydrophobic domain as a membrane anchor. Therefore, differential centrifugation experiments were conducted to investigate whether AtVTI1a was associated with membranes. The majority of the AtVTI1a protein was precipitated at 8000 × *g*, and no AtVTI1a remained in the supernatant after centrifugation at 100,000 × *g* (Figure 5B). To confirm that AtVTI1a is an integral membrane protein, various treatments that affect the membrane association of peripheral proteins were applied to total membranes from *Arabidopsis* suspension cells. The membranes were pelleted afterward, and the amounts of AtVTI1a in the supernatants were compared with those in the starting material. AtVTI1a was not stripped from the membrane by 2 M urea, 1 M NaCl, or 0.1 M Na_2CO_3, conditions that dissociate peripheral proteins from membranes (Figure 5C). AtVTI1a was solubilized by detergents, indicating that it is an integral membrane protein.

Cofractionation of AtVTI1a and Other Markers in Sucrose Density Gradients

To determine the subcellular localization of AtVTI1a, we performed a sucrose density step gradient analysis. Postnuclear supernatant from 3-wk-old *Arabidopsis* cultured roots was loaded on top of a step sucrose gradient (15, 24, 33, 40, and 54% from top to bottom). The gradient was equilibrated by ultracentrifugation at 100,000 × *g* for 3 h at 4°C, and fractions of 0.5 ml were collected from the top to the bottom. The sucrose density distribution was close to linear after the centrifugation step (Figure 6B). Fractions were then analyzed by immunoblotting. The fractionation of AtVTI1a was compared with three other subcellular marker proteins, as shown in Figure 6A. AtVTI1a cofractionated with AtPEP12p, which peaked at 36.5 and 54.4%; AtELP mostly cofractionated with AtVTI1a, with peaks at densities of 36.5 and 54.4%. A separate peak of AtELP was also observed at a sucrose concentration of 32.2%. The vacuolar tonoplast marker H^+PPase (Maeshima *et al*., 1994) fractionated at the top of the gradient, separated from AtVTI1a and other

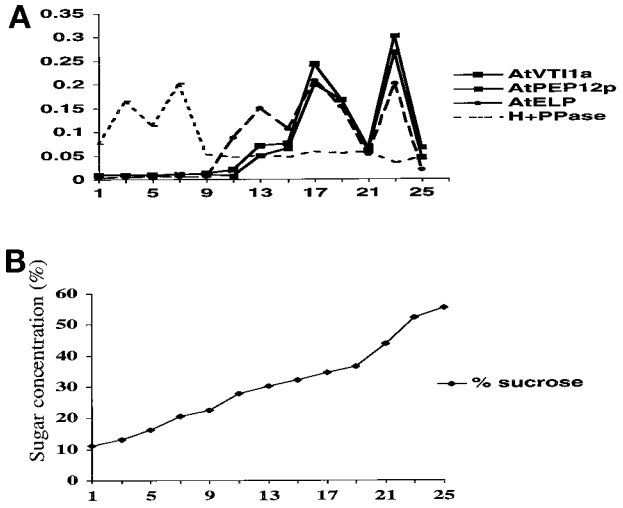

Figure 6. Subcellular fractionation of AtVTI1a by step sucrose gradient. Postnuclear membranes of *Arabidopsis* roots were loaded on a step sucrose gradient. After equilibrium by ultracentrifugation at 100,000 × *g* for 3 h, 0.5-ml fractions were collected from top (1) to bottom of the gradient (25). Equal volumes of odd-numbered fractions were loaded on an SDS-PAGE gel and immunoblotted with anti-AtVTI1a, anti-AtELP, anti-AtPEP12p, and anti-H^+PPase antibodies. Blots were analyzed by densitometry, and the percentage of the total marker protein detected in each fraction for AtVTI1a, AtPEP12p, AtELP, and H^+PPase was plotted in A. The sucrose concentration of each fraction was determined by refractometry and plotted in B.

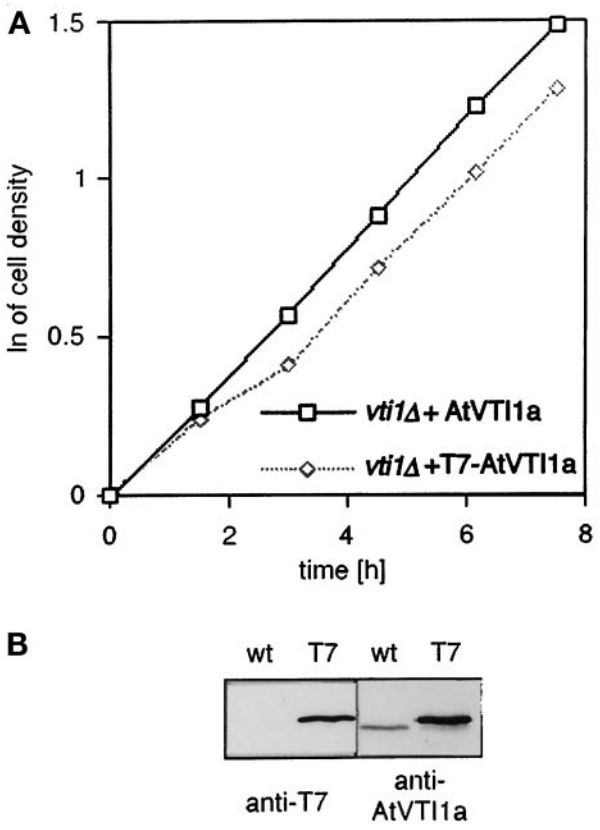

Figure 7. T7 tag does not affect AtVTI1a function and is expressed in transgenic plants. (A) Growth curves of *vti1*Δ cells expressing AtVTI1a or T7-AtVTI1a. *vti1*Δ cells (FvMY6) expressing either AtVTI1a or epitope-tagged T7-AtVTI1a grew at similar rates, indicating that T7-AtVTI1a was functional. Cells were grown in a rich medium at 30°C at logarithmic phase. The cell density was determined by measuring the optical density at 600 nm. (B) T7 antibodies specifically recognized T7-AtVTI1a in transgenic plants. Equal amounts of postnuclear supernatant of *Arabidopsis* (T7-AtVTI1a transgenic plants or wild-type) were separated on SDS-PAGE gel and immunoblotted with monoclonal T7 antibody or polyclonal antiserum against AtVTI1a raised in guinea pig.

marker proteins. These data suggest that AtVTI1a does not reside on the tonoplast membrane but, rather, cofractionates with AtPEP12 on the PVC or with AtELP on the TGN and the PVC.

T7-tagged AtVTI1a Behaves Similarly to Endogenous AtVTI1a in Yeast and in Plants

To further differentiate the two AtVTI1 proteins and investigate AtVTI1a specifically, an 11–amino acid T7 tag was fused at the N terminus of AtVTI1a. The behavior of this tagged version of AtVTI1a was first compared with wild-type AtVTI1a in yeast and plants. T7-AtVTI1a was expressed in yeast to determine whether the epitope-tagged protein retained function. The growth behavior of *vti1*Δ cells (FvMY6) expressing either AtVTI1a or T7-AtVTI1a was compared by measuring the optical density of cultures growing in logarithmic phase (Figure 7A). These two strains grew at similar rates and had doubling times of ~3.5 h. These data indicated that the T7-tagged AtVTI1a was functional in yeast.

The T7-tagged *AtVTI1a* was transformed into *Arabidopsis* ecotype Columbia. One of the transgenic lines expressing medium amounts of T7-AtVTI1a was chosen for further study. On a Western blot, in addition to endogenous AtVTI1a migrating at 28 kDa, AtVTI1a antibodies also detected a protein band migrating at ~29 KDa, which was also recognized by monoclonal T7 antibody (Figure 7B). Thus this 29-kDa protein band was determined to be T7-tagged AtVTI1a. T7 antibody did not recognize any other protein bands in extracts from either the transgenic or wild-type line (Figure 7B), suggesting that these antibodies were specific in *Arabidopsis*. Because we lacked any functional assay for AtVTI1a in plants, the fractionation patterns of tagged and endogenous AtVTI1a on sucrose density gradients were compared. No differences in fractionation patterns were observed between tagged and endogenous AtVTI1a in transgenic plants or between the fractionation pattern of tagged AtVTI1a in transgenic plants and endogenous AtVTI1a in wild-type

plants (our unpublished results). There were also no observable phenotypic differences between the transgenic plants and wild-type plants (our unpublished results). These data indicate that T7-AtVTI1a expressed in plants behaves indistinguishably from endogenous AtVTI1a, and the expression of tagged protein does not affect the physiology of the plant.

Cytochemical Analysis of T7-tagged AtVTI1a in Transgenic Plants

We have shown above that AtVTI1a cofractionated with AtPEP12p and AtELP on a sucrose step density gradient. Therefore, we attempted to further investigate the subcellular localization of AtVTI1a and the relationship between AtVTI1a and AtPEP12p or AtELP by immunocytochemistry. We found that AtVTI1a antiserum was unsuitable for these studies, probably because of low amounts of endogenous protein and loss of antigenicity during fixation. However, the T7-tagged AtVTI1a transgenic plants allowed us to study the localization of AtVTI1a in the cell and to perform double labeling experiments with other membrane markers. The majority of the T7-AtVTI1a–associated labeling was found on the TGN (Figure 8A) and on electron-dense, uncoated vesicular structures that were often found near the Golgi of the root cells (Figure 8B). We performed statistical analysis of many independent micrographs showing T7-AtVTI1a localization. This analysis indicated that the distribution of T7-VTI1a was evenly split between TGN (51%) and dense vesicles (49%). The orientation of the Golgi was determined based on appearance and the more electron-dense staining pattern of the *trans*-Golgi and the TGN. Almost no T7-AtVTI1a was found on the cytoplasm, endoplasmic reticulum, nuclei, or plasma membrane (our unpublished results), and control sections showed almost no background (Figure 8C).

Our fractionation experiments indicated that AtVTI1a partially cofractionated with AtELP, suggesting at least partial colocalization. To analyze this possibility directly, we performed double-labeling experiments on T7-AtVTI1a plants. AtVTI1a was first labeled with specific mAb against T7 and detected with 10-nm gold. A second fixation and blocking step was then performed before incubating the sections with antiserum specific to AtELP, followed by detection with 5-nm gold. It was observed that both T7 mAb and AtELP antiserum specifically labeled the TGN compartment (Figure 8D) and electron-dense structures (Figure 8E). In control experiments we substituted preimmune serum for one of the primary antibodies. An example of one of these experiments is shown in Figure 8F. In this case, sections were labeled with T7 antibody, followed by preimmune serum instead of AtELP antibody. No labeling of any structures with 5-nm gold was seen; however, T7-AtVTI1a labeling was present on the TGN. The converse experiments were also done omitting the T7 antibody. Again, no labeling with 10-nm gold was seen. Also, no labeling of the TGN and dense structures was seen in the absence of both primary antisera but with the secondary antibodies decorated with 5- and 10-nm gold (our unpublished results).

We speculate that the electron-dense vesicles labeled with T7-AtVTI1a are PVCs. AtPEP12p is the only known marker on the PVC. Therefore, similar double EM immunocytochemistry was performed to colocalize T7-AtVTI1a and AtPEP12p. For this localization, ultrathin cryosections were used because AtPEP12p could not be localized using embedment into conventional resin (Conceição *et al.*, 1997). The incubation procedure was similar to that of the T7-AtVTI1a and AtELP double labeling except that AtPEP12p antiserum was used instead of AtELP antiserum. Analysis of sections revealed that T7-AtVTI1a and AtPEP12p colocalized to the structures that are typical for the PVC (Figure 9, A and B) (Sanderfoot *et al.*, 1998). No staining of the PVC was seen in control experiments (Figure 9C). Together with the yeast complementation data, these results strongly support our proposal that AtVTI1a is a v-SNARE involved in traffic between the Golgi and the PVC.

AtVTI1a Interacts with AtPEP12p

To further investigate whether AtVTI1a interacts with a t-SNARE in vivo, we attempted to immunoprecipitate AtVTI1a from plant cell extracts and identify the coimmunoprecipitated proteins. Cultured roots of T7-AtVTI1a plants or wild-type plants were homogenized, and the extract was clarified by centrifugation at 1000 $\times$ *g* for 10 min at 4°C. Triton X-100 was added to the supernatant to a final concentration of 1% to solubilize the membrane proteins. These lysates were incubated with T7 antibody conjugated to agarose beads. The beads were washed, and the bound proteins were eluted. Samples of total extracts, flow-through, and eluate were separated on SDS-PAGE. The separated proteins were then transferred to a nitrocellulose membrane and blotted by various antibodies. T7-AtVTI1a bound to the T7 antibody agarose with high efficiency (Figure 10). Significantly, a fraction of the total AtPEP12p was coprecipitated with T7-AtVTI1a in the eluate. (Figure 10, right side) As we expected, in the control experiment in which wild-type plant extract was used (Figure 10, left side), AtVTI1a did not bind to the T7 antibody. Accordingly, AtPEP12p was not found in the eluate. Thus, our data indicate that AtPEP12p was associated specifically with T7-AtVTI1a. In contrast, AtELP was not copurified by T7 antibody agarose. These coimmunoprecipitation experiments strongly suggest that AtVTI1a

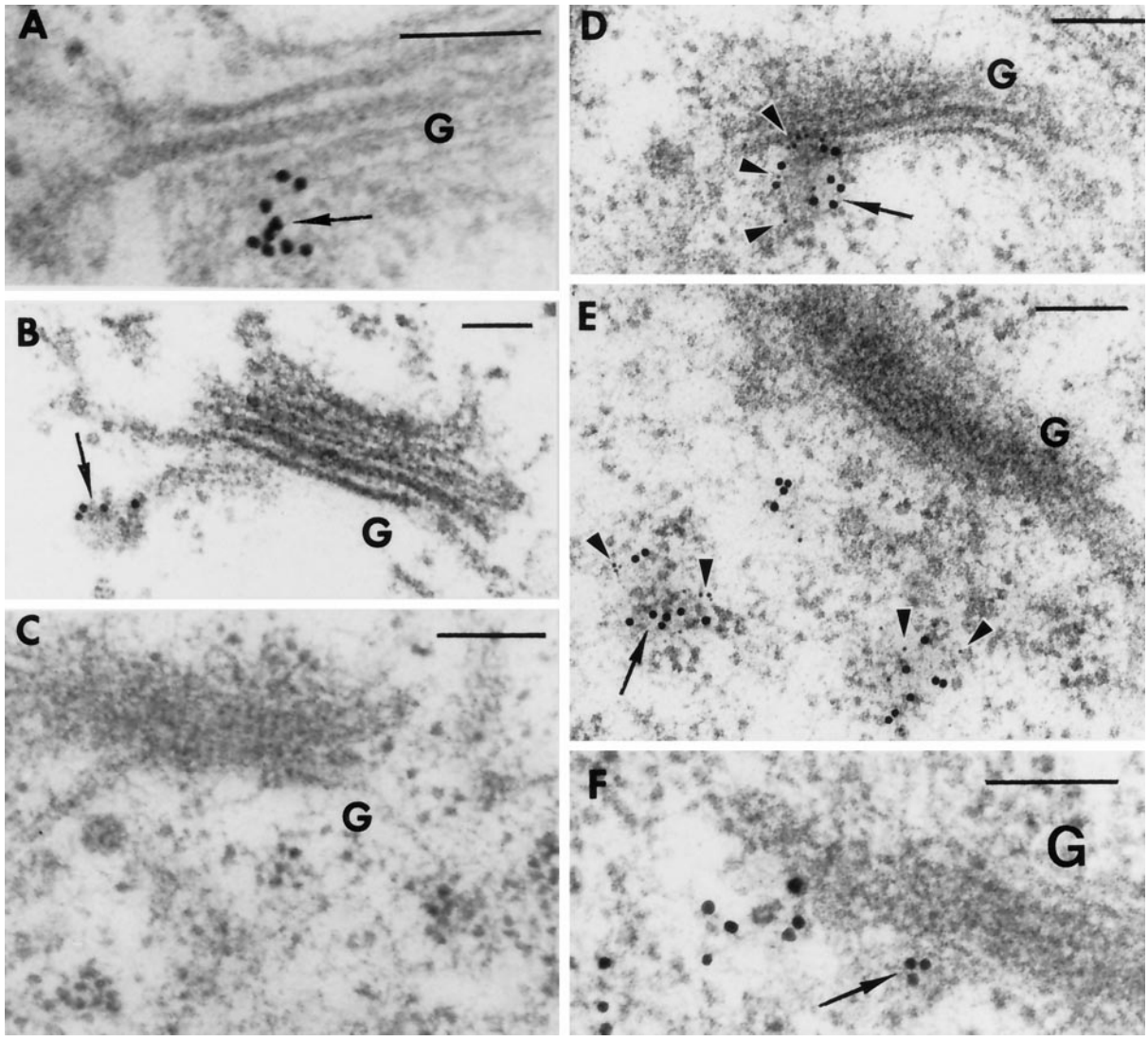

Figure 8. In situ localization of T7-AtVTI1a and AtELP on ultrathin sections of *Arabidopsis* roots from T7-AtVTI1a transgenic plants. T7-AtVTI1a and AtELP are localized on the TGN and on dense vesicles. (A and B) Ultrathin sections were incubated with T7 mAb followed by rabbit anti-mouse IgG and biotinylated goat anti-rabbit secondary antibody and were visualized with streptavidin conjugated to 10-nm colloidal gold. (C) Control. The ultrathin sections were treated with the same procedure as described in A and B, except T7 mAb was substituted with 2% BSA in PBS. T7-AtVTI1a and AtELP are colocalized on the TGN (D) and on dense vesicles (E). (D and E) Ultrathin sections were incubated with T7 mAb followed by rabbit anti-mouse IgG and biotinylated goat anti-rabbit secondary antibody and were visualized with streptavidin conjugated to 10-nm colloidal gold. After the second fixation step (see MATERIALS AND METHODS), the same sections were incubated with antiserum to AtELP, followed by biotinylated goat anti-rabbit secondary antibody, and then visualized with streptavidin conjugated to 5-nm colloidal gold. (F) Control section. The same procedures were used as in D and E, except preimmune serum was used in the place of AtELP antiserum. G, Golgi; arrow, AtVTI1a; arrowhead, AtELP; bar, 0.1 μm.

forms a Triton X-100–resistant SNARE complex with AtPEP12p in vivo.

DISCUSSION

Several pathways to the vacuole have been identified in yeast. Vti1p, a multifunctional v-SNARE, has been shown to be involved in numerous pathways to the vacuole, including the CPY pathway via the PVC, the ALP alternative pathway, and the CVT pathway for vacuole taking cytosolic proteins such as API (Fischer von Mollard *et al.*, 1997; Holthuis *et al.*, 1998; Fischer von Mollard and Stevens, 1999). We have identified two *Arabidopsis VTI1* homologues. The deduced amino acid sequences of these two genes share significant similarity to Vti1p found in yeast and mammals

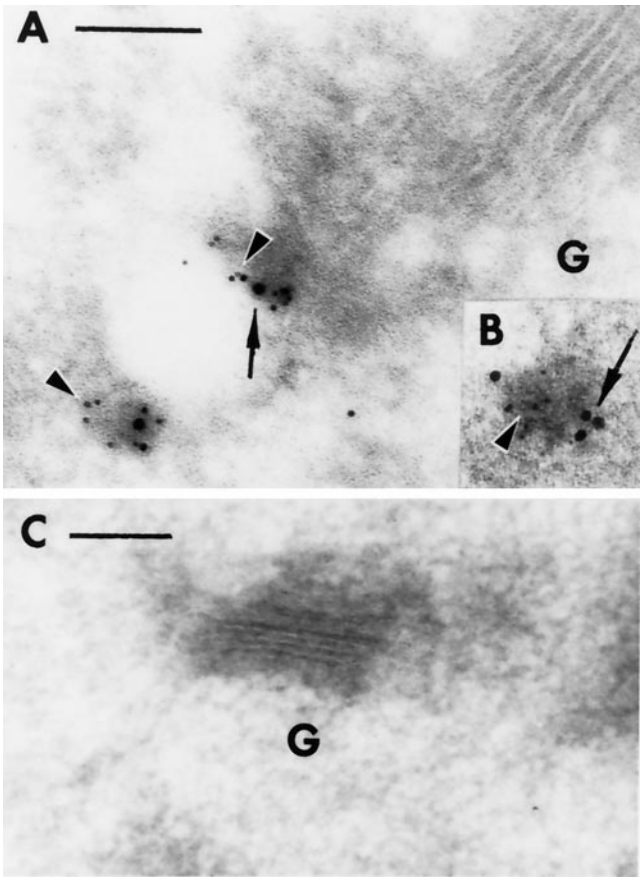

Figure 9. T7-AtVTI1a and AtPEP12p colocalize on the PVC in cryosections of *Arabidopsis* roots from T7-AtVTI1a transgenic plants. (A and B) Ultrathin sections were incubated with T7 mAb followed by rabbit anti-mouse IgG and biotinylated goat anti-rabbit secondary antibody and were visualized with streptavidin conjugated to 10-nm colloidal gold. After the second fixation step (see MATERIALS AND METHODS), the same sections were incubated with AtPEP12p antiserum, followed by biotinylated goat anti-rabbit IgG, and then detected by streptavidin conjugated to 5-nm gold particles. (C) Control section. The same procedures were used as in A and B, except first antibodies were substituted with 2% BSA in PBS for T7 mAb and AtPEP12p preimmune serum for AtPEP12p antiserum. G, Golgi; arrow, AtVTI1a; arrowhead, AtPEP12p; bar, 0.1 μm.

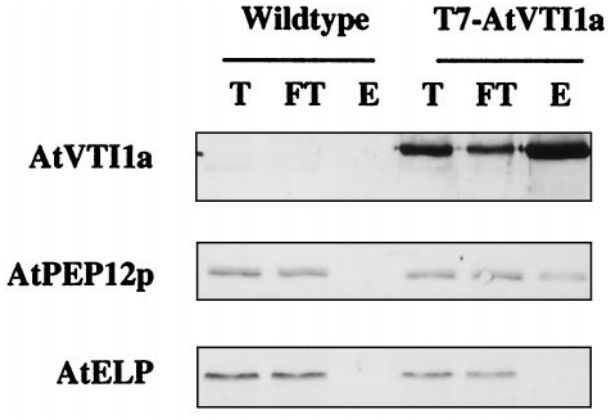

Figure 10. AtVTI1a associates with AtPEP12p. Postnuclear supernatant from three grams of T7-AtVTI1a transgenic or wild-type *Arabidopsis* plants (21 d old) were treated with 1% Triton X-100 to solubilize membrane proteins. An aliquot was saved as total protein. The Triton X-100–solubilized protein extract was then incubated with 100 μl of T7 antibody agarose (Novagen) for 5 h. Beads were pelleted, and the flow-through was collected. After being washed, proteins associated with the T7 antibody agarose were eluted. Equal volumes of total (T), flow-through (FT), and eluate (E) were separated by SDS-PAGE, followed by immunoblotting with antibodies against AtVTI1a, AtPEP12p, or AtELP.

(Fischer von Mollard *et al*., 1997; Lupashin *et al*., 1997; Advani *et al*., 1998; Fischer von Mollard and Stevens 1998; Li *et al*., 1998). We have found that AtVTI1a and AtVTI1b were able to substitute for yeast Vti1p in different membrane transport pathways. AtVTI1a efficiently suppressed the CPY mistargeting and the growth defect in one set of *vti1* temperature-sensitive mutants and in *vti1* null mutants, suggesting that AtVTI1a could substitute functionally for yeast Vti1p in these pathways. On the other hand, rather than rescuing the CPY missorting phenotype, AtVTI1b was found to restore transport of 1) the vacuolar protein ALP that is transported through the Golgi but bypasses the PVC and 2) the hydrolase API, which uses the CVT pathway from the cytoplasm to the vacuole. By contrast, AtVTI1a does not function in the ALP or API transport pathway in yeast.

Whereas there is only one *VTI1* gene in yeast, two *VTI1*-related genes have been identified in *Arabidopsis*, mouse and human. It is speculated that the existence of two paralogues reflected greater complexity of the endomembrane system in higher organisms compared with yeast. In other words, various members of the Vti1 gene family probably have different functions. This notion is supported by the recent report that the two mouse *VTI1* genes are expressed ubiquitously and the mouse Vti1 proteins may be localized on different compartments (Xu *et al*., 1998). Whereas the mouse paralogues share only 30% amino acid identity (Lupashin *et al*., 1997), the plant paralogues are more closely related and share 60% amino acid identity. RNA analysis in plants using gene-specific probes did not detect any expression pattern difference between these two genes, indicating that both genes are expressed in the same cells and do not represent organ-specific isoforms. However, the intracellular location of the AtVTI1b protein is not yet known. In yeast, the two *Arabidopsis* Vti1 homologues have functionally substituted for yVti1p in different vesicle transport steps. In plants, AtVTI1a most likely functions in a transport pathway analogous to the CPY pathway (see below). Based on yeast complementation data, we propose that AtVTI1b is involved in different vacuolar transport pathways in plants. However, the specific function of the two *VTI1* genes in plants will be revealed

only when we are able to investigate their products at the protein level.

In plants, several components of the vacuolar targeting pathway machinery have been identified. AtPEP12p is a t-SNARE that resides on the PVC (Conceição *et al.*, 1997). AtELP is proposed to be a vacuolar protein-sorting receptor. In previous studies it has been demonstrated that AtPEP12p and AtELP colocalize on the PVC; AtELP has also been found in the Golgi and the TGN (Sanderfoot *et al.*, 1998). Because it is highly probable that both of these proteins are involved in mediating transport of soluble vacuolar proteins, their intracellular distribution in relation to AtVTI1a was very revealing. Under EM, T7-AtVTI1a was localized on the TGN and on vesicular structures that most likely compose the PVC. By double labeling, AtVTI1a was found to colocalize with AtELP at the TGN and with AtPEP12p at the PVC. The colocalization of these three proteins suggests that AtVTI1a, AtELP, and AtPEP12p are most likely involved in the same pathway, the pathway responsible for the transport of a subset of vacuolar proteins at the step between the TGN and the PVC. Coimmunoprecipitation of AtVTI1a and AtPEP12p strongly supports the hypothesis that AtVTI1a, as a v-SNARE, is responsible for the docking of vesicles from the TGN to the PVC by interacting with AtPEP12p, the PVC t-SNARE. It will be interesting to characterize the vesicles whose fusion is controlled by AtVTI1a and to define the branches of the plant membrane traffic pathways in which AtVTI1a is involved. Further investigations should also reveal the membrane traffic pathways regulated by AtVTI1b.

ACKNOWLEDGMENTS

We acknowledge Drs. Anton Sanderfoot and Diane Bassham for valuable critiques and comments on the manuscript. We thank Gyu-in Lee for help on Northern analyses of *AtVTI1a* and *AtVTI1b*. N.V.R. is supported by National Science Foundation grant MCB-950730 and US Department of Energy grant DE-FG02-91ER-20021; T.H.S. is supported by National Institutes of Health grant GM 32448.

REFERENCES

Advani, R.J., Bae, H.R., Bock, J.B., Chao, D.S., Doung, Y.C., Prekeris, R., Yoo, J.S., and Scheller, R.H. (1998). Seven novel mammalian SNARE proteins localize to distinct membrane compartments. J. Biol. Chem. *273*, 10317–10324.

Ahmed, S.U., Bar-Peled, M., and Raikhel, N.V. (1997). Cloning and subcellular location of an *Arabidopsis* receptor-like protein that shares common features with protein-sorting receptors of eukaryotic cells. Plant Physiol. *114*, 325–336.

Altschul, S.F., Gish, W., Miller, W., Myers, E.W., and Lipman, D.J. (1990). Basic local alignment search tool. J. Mol. Biol. *215*, 403–410.

Bar-Peled, M., and Raikhel, N.V. (1997). Characterization of AtSEC12 and AtSAR1. Proteins likely involved in endoplasmic reticulum and Golgi transport. Plant Physiol. *114*, 315–324.

Bassham, D.C., Gal, S., Conceição, A.S., and Raikhel, N.V. (1995). An *Arabidopsis* syntaxin homologue isolated by functional complementation of a yeast pep12 mutant. Proc. Natl. Acad. Sci. USA *92*, 7262–7266.

Bassham, D.C., and Raikhel, N.V. (1997). Molecular aspects of vacuole biogenesis. Adv. Bot. Res. *25*, 43–58.

Becherer, K.A., Rieder, S.E., Emr, S.D., and Jones, E.W. (1996). Novel syntaxin homologue, Pep12p, required for the sorting of lumenal hydrolases to the lysosome-like vacuole in yeast. Mol. Biol. Cell *7*, 579–594.

Bent, A.F., Kunkel, B.N., Dahlbeck, D., Brown, K.L., Schmidt, R., Giraudat, J., Leung, J., and Staskawicz, B.J. (1994). RPS2 of *Arabidopsis thaliana*: a leucine-rich repeat class of plant disease resistance genes. Science *265*, 1856–1860.

Bryant, N.J., and Stevens, T.H. (1998). Vacuole biogenesis in *Saccharomyces cerevisiae:* protein transport pathways to the yeast vacuole. Microbiol. Mol. Biol. Rev. *62*, 230–247.

Calakos, N., Bennett, M.K., Peterson, K.E., and Scheller, R.H. (1994). Protein-protein interactions contributing to the specificity of intracellular vesicular trafficking. Science *263*, 1146–1149.

Conceição, S.A., Marty-Mazars, D., Bassham, D.C., Sanderfoot, A.A., Marty, F., and Raikhel, N.V. (1997). The syntaxin homolog AtPEP12p resides on a late postGolgi compartment in plants. Plant Cell *9*, 571–582.

Cowles, C.R., Odorizzi, G., Payne, G.S., and Emr, S.D. (1997a). The AP-3 adaptor complex is essential for cargo-selective transport to the yeast vacuole. Cell *91*, 109–118.

Cowles, C.R., Snyder, W.B., Burd, C.G., and Emr, S.D. (1997b). Novel Golgi to vacuole delivery pathway in yeast: identification of a sorting determinant and required transport component. EMBO J. *16*, 2769–2782.

Darsow, T., Rieder, S.E., and Emr, S.D. (1997). A multispecificity syntaxin homologue, Vam3p, essential for autophagic and biosynthetic protein transport to the vacuole. J. Cell Biol. *138*, 517–529.

Fischer von Mollard, G., Nothwehr, S.F., and Stevens, T.H. (1997). The yeast v-SNARE Vti1p mediates two vesicle transport pathways through interactions with the t-SNAREs Sed5p and Pep12p. J. Cell Biol. *137*, 1511–1524.

Fischer von Mollard, G., and Stevens, T.H. (1998). A human homolog can functionally replace the yeast vesicle-associated SNARE Vti1p in two vesicle transport pathways. J. Biol. Chem. *273*, 2624–2630.

Fischer von Mollard, G., and Stevens, T.H. (1999). The *Saccharomyces cerevisiae* v-SNARE Vti1p is required for multiple membrane transport pathways to the vacuole. Mol. Biol. Cell *10*, 1719–1732.

Gomez, L., and Chrispeels, M.J. (1993). Tonoplast and soluble vacuolar proteins are targeted by different mechanisms. Plant Cell *5*, 1113–1124.

Hanson, P.I., Heuser, J.E., and Jahn, R. (1997). Neurotransmitter release—four years of SNARE complexes. Curr. Opin. Neurobiol. *7*, 310–315.

Hay, J.C., and Scheller, R.H. (1997). SNAREs and NSF in targeted membrane fusion. Curr. Opin. Cell Biol. *9*, 505–512.

Hayashi, T., McMahon, H., Yamasaki, S., Binz, T., Hata, Y., Sudhof, T.C., and Niemann, H. (1994). Synaptic vesicle membrane fusion complex: action of clostridial neurotoxins on assembly. EMBO J. *13*, 5051–5061.

Holthuis, J.C., Nichols, B.J., Dhruvakumar, S., and Pelham, H.R. (1998). Two syntaxin homologues in the TGN/endosomal system of yeast. EMBO J. *17*, 113–126.

Jones, E.W. (1977). Proteinase mutants of *Saccharomyces cerevisiae*. Genetics *85*, 23–33.

Kirsch, T., Paris, N., Butler, J.M., Beevers, L., and Rogers, J.C. (1994). Purification and initial characterization of a potential plant vacuolar targeting receptor. Proc. Natl. Acad. Sci. USA *91*, 3403–3407.

Kirsch, T., Saalbach, G., Raikhel, N.V., and Beevers, L. (1996). Interaction of a potential vacuolar targeting receptor with amino- and carboxyl-terminal targeting determinants. Plant Physiol. *111*, 469–474.

Klionsky, D.J. (1998). Nonclassical protein sorting to the yeast vacuole. J. Biol. Chem. *273*, 10807–10810.

Klionsky, D.J., Cueva, R., and Yaver, D.S. (1992). Aminopeptidase I of *Saccharomyces cerevisiae* is localized to the vacuole independent of the secretory pathway. J. Cell Biol. *119*, 287–299.

Klionsky, D.J., and Emr, S.D. (1989). Membrane protein sorting: biosynthesis, transport and processing of yeast vacuolar alkaline phosphatase. EMBO J. *8*, 2241–2250.

Kyte, J., and Doolittle, R.F. (1982). A simple method for displaying the hydropathic character of a protein. J. Mol. Biol. *157*, 105–132.

Li, H.C., Tahara, H., Tsuyama, N., and Ide, T. (1998). A hVti1 homologue: its expression depends on population doubling levels in both normal and SV40-transformed human fibroblasts. Biochem. Biophys. Res. Commun. *247*, 70–74.

Lukowitz, W., Mayer, U., and Jürgens, G. (1996). Cytokinesis in the *Arabidopsis* embryo involves the syntaxin-related KNOLLE gene product. Cell *84*, 61–71.

Lupashin, V.V., Pokrovskaya, I.D., McNew, J.A., and Waters, M.G. (1997). Characterization of a novel yeast SNARE protein implicated in Golgi retrograde traffic. Mol. Biol. Cell *8*, 2659–2676.

Maeshima, M., Hara-Nishimura, I., Takeuchi, Y., and Nishimura, M. (1994). Accumulation of vacuolar H^+-pyrophosphatase and H^+-ATPase during reformation of the central vacuole in germinating pumpkin seeds. Plant Physiol. *106*, 61–69.

Maeshima, M., and Yoshida, S. (1989). Purification and properties of vacuolar membrane proton-translocating inorganic pyrophosphatase from mung bean. J. Biol. Chem. *264*, 20068–20073.

Matsuoka, K., Bassham, D.C., Raikhel, N.V., and Nakamura, K. (1995). Different sensitivity to wortmannin of two vacuolar sorting signals indicates the presence of distinct sorting machineries in tobacco cells. J. Cell Biol. *130*, 1307–1318.

Nothwehr, S.F., Roberts, C.J., and Stevens, T.H. (1993). Membrane protein retention in the yeast Golgi apparatus: dipeptidyl aminopeptidase A is retained by a cytoplasmic signal containing aromatic residues. J. Cell Biol. *121*, 1197–1209.

Odorizzi, G., Cowles, C.R., and Emr, S.D. (1998). The AP-3 complex, a coat of many colors. Trends Cell Biol. *8*, 282–288.

Piper, R.C., Bryant, N.J., and Stevens, T.H. (1997). The membrane protein alkaline phosphatase is delivered to the vacuole by a route that is distinct from the VPS-dependent pathway. J. Cell Biol. *138*, 531–545.

Robinson, J.S., Klionsky, D.J., Banta, L.M., and Emr, S.D. (1988). Protein sorting in *Saccharomyces cerevisiae*: isolation of mutants defective in the delivery and processing of multiple vacuolar hydrolases. Mol. Cell. Biol. *8*, 4936–4948.

Sambrook, J., Fritsch, E.F., and Maniatis, T. (1989). Molecular Cloning: A Laboratory Manual, 2nd ed., Plainview, NY: Cold Spring Harbor Laboratory Press, 7.37–7.57.

Sanderfoot, A.A., Ahmed, S.U., Marty-Mazars, D., Rapoport, I., Kirchhausen, T., Marty, F., and Raikhel, N.V. (1998). A putative vacuolar cargo receptor partially colocalizes with AtPEP12p on a prevacuolar compartment in *Arabidopsis* roots. Proc. Natl. Acad. Sci. USA *95*, 9920–9925.

Sato, M.H., Nakamura, N., Ohsumi, Y., Kouchi, H., Kondo, M., Hara-Nishimura, I., Nishimura, M., and Wada, Y. (1997). The AtVAM3 encodes a syntaxin-related molecule implicated in the vacuolar assembly in *Arabidopsis thaliana*. J. Biol. Chem. *272*, 24530–24535.

Shimada, T., Kuroyanagi, M., Nishimura, M., and Hara-Nishimura, I. (1997). A pumpkin 72-kDa membrane protein of precursor-accumulating vesicles has characteristics of a vacuolar sorting receptor. Plant Cell Physiol. *38*, 1414–1420.

Slot, J.W., Geuze, H.J., Gigengack, S., Lienhard, G.E., and James, D.E. (1991). Immuno-localization of the insulin regulatable glucose transporter in brown adipose tissue of the rat. J. Cell Biol *113*, 123–135.

Söllner, T., Bennett, M.K., Whiteheart, S.W., Scheller, R.H., and Rothman, J.E. (1993). A protein assembly-disassembly pathway in vitro that may correspond to sequential steps of synaptic vesicle docking, activation, and fusion. Cell *75*, 409–418.

Srivastava, A., and Jones, E.W. (1998). Pth1/Vam3p is the syntaxin homolog at the vacuolar membrane of *Saccharomyces cerevisiae* required for the delivery of vacuolar hydrolases. Genetics *148*, 85–98.

Stepp, J.D., Huang, K., and Lemmon, S.K. (1997). The yeast adaptor protein complex, AP-3, is essential for the efficient delivery of alkaline phosphatase by the alternate pathway to the vacuole. J. Cell Biol. *139*, 1761–1764.

Stevens, T., Esmon, B., and Schekman, R. (1982). Early stages in the yeast secretory pathway are required for transport of carboxypeptidase Y to the vacuole. Cell *30*, 439–448.

Sutton, R.B., Fasshauer, D., Jahn, R., and Brunger, A.T. (1998). Crystal structure of a SNARE complex involved in synaptic exocytosis at 2.4 Å resolution. Nature *395*, 347–353.

Tokuyasu, K.T. (1989). Use of poly(vinylpyrrolidone) and poly(vinyl alcohol) for cryoultramicrotomy. Histochem. J. *21*, 163–171.

Vater, C.A., Raymond, C.K., Ekena, K., Howald-Stevenson, I., and Stevens, T.H. (1992). The VPS1 protein, a homolog of dynamin required for vacuolar protein sorting in *Saccharomyces cerevisiae*, is a GTPase with two functionally separable domains. J. Cell Biol. *119*, 773–786.

Vernet T., Dignard, D., and Thomas, D.Y. (1987). A family of yeast expression vectors containing the phage f1 intergenic region. Gene *52*, 225–233.

Wada, Y., Nakamura, N., Ohsumi, Y., and Hirata, A. (1997). Vam3p, a new member of syntaxin related protein, is required for vacuolar assembly in the yeast *Saccharomyces cerevisiae*. J. Cell Sci. *110*, 1299–1306.

Xu, Y., Wong, S.H., Tang, B.L., Subramaniam, V.N., Zhang, T., and Hong, W. (1998). A 29-kilodalton Golgi soluble *N*-ethylmaleimide-sensitive factor attachment protein receptor (Vti1-rp2) implicated in protein trafficking in the secretory pathway. J. Biol. Chem. *273*, 21783–21789.

Zheng, H., Bassham, D.C., Conceição, A.S., and Raikhel, N.V. (1999). The syntaxin family of proteins in *Arabidopsis*: a new syntaxin homologue shows polymorphism between two ecotypes. J. Exp. Bot. (*in press*).